Journal of Coordination Chemistry

ISSN: 0095-8972 (Print) 1029-0389 (Online) Journal homepage: http://www.tandfonline.com/loi/gcoo20

Synthesis, crystal structures, DNA binding, and cytotoxicity activities of two copper(II) complexes based on unsymmetrical tripodal ligands

Xiao-Tong Zhang, Zhong-Ying Ma, Chuan Zhao, Qi-Ji Zhou, Cheng-Zhi Xie & Jing-Yuan Xu

To cite this article: Xiao-Tong Zhang, Zhong-Ying Ma, Chuan Zhao, Qi-Ji Zhou, Cheng-Zhi Xie & Jing-Yuan Xu (2015) Synthesis, crystal structures, DNA binding, and cytotoxicity activities of two copper(II) complexes based on unsymmetrical tripodal ligands, Journal of Coordination Chemistry, 68:13, 2307-2323, DOI: 10.1080/00958972.2015.1040781

To link to this article: http://dx.doi.org/10.1080/00958972.2015.1040781

Accepted author version posted online: 15 Apr 2015.
Published online: 16 Jun 2015.

Journal of Coordination Chemistry, 2015
Vol. 68, No. 13, 2307–2323, http://dx.doi.org/10.1080/00958972.2015.1040781

Synthesis, crystal structures, DNA binding, and cytotoxicity activities of two copper(II) complexes based on unsymmetrical tripodal ligands

XIAO-TONG ZHANG†, ZHONG-YING MA†, CHUAN ZHAO‡, QI-JI ZHOU†,[1], CHENG-ZHI XIE*† and JING-YUAN XU*†

†Tianjin Key Laboratory on Technologies Enabling Development of Clinical Therapeutics and Diagnostics, School of Pharmacy, Tianjin Medical University, Tianjin, PR China
‡China Research Center of Basic Medical Sciences, Tianjin Medical University, Tianjin, China

(*Received 20 July 2014; accepted 18 March 2015*)

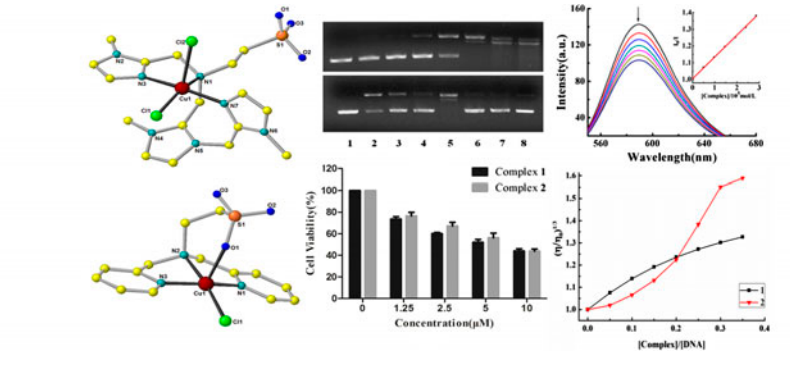

[Cu(L1)Cl$_2$]·3H$_2$O (**1**) and [Cu(L2)Cl]·2H$_2$O (**2**) based on new unsymmetrical tripodal ligands (L1 = {(N-methyl-imidazolylmethyl)[N-methyl-N-(N-methyl-imidazolylmethyl)imidazolylmethyl] amino}ethanesulfonic acid, L2 = [bis(2-pyridylmethyl)amino]ethanesulfonic acid) have been synthesized and characterized by elemental analysis, IR, and single-crystal X-ray diffraction. In the discrete mononuclear structures of **1** and **2**, copper is five-coordinate in a distorted trigonal bipyramidal structure. Interaction of the complexes with CT-DNA was investigated by UV–vis spectra, fluorescence spectra, and viscosity; the data reveal that **1** and **2** bind to CT-DNA by partial intercalation. Gel electrophoresis assays demonstrate that these two complexes display efficient oxidative cleavage of supercoiled DNA in the presence of H_2O_2, and MTT assays indicated that both **1** and **2** showed significant cytotoxicity toward human hepatoma cell HepG-2.

Keywords: Mononuclear; Copper(II) complex; Tripodal ligand; DNA interaction; Cytotoxicity

*Corresponding authors. Email: xiechengzhi@tmu.edu.cn (C.-Z. Xie); xujingyuan@tmu.edu.cn (J.-Y. Xu)
[1]Present address: Department of Pharmacy, Affiliated Hospital of Youjiang Medical College for Nationalities, Baise, Guangxi, PR China.

1. Introduction

DNA is the primary target for most anticancer and antiviral therapies, and thus, investigation of interactions of DNA with small molecules is very important in the development of cancer chemotherapy. Many studies indicate that metal complexes can interact noncovalently with DNA by three modes, intercalation, groove binding, and external electrostatic, of which the intercalation is considered as the most effective mode, because molecules with extended planar aromatic systems can be inserted between DNA base pairs via π–π stacking, stabilizing, lengthening, stiffening, and unwinding the double helix of DNA [1–6]. As widely used metal-based antitumor drugs targeting DNA, platinum complexes, such as cisplatin, carboplatin, and oxaliplatin, have achieved success in cancer therapeutics. However, resistance and toxic side effects of these Pt-based drugs urge scientists to find alternative agents [7–10]. As metal-based anticancer substances, copper complexes have emerged for their bio-essential activity and oxidative nature [11]. Furthermore, Cu(II) complexes are capable of interacting with DNA while their ability of binding to, and cleaving DNA, depends on the coordinated ligand [12–14].

Interest in tripodal ligands, such as tris[(2-pyridyl)methyl]amine (tpa) as well as derivatives, stems from their tenability and flexibility in structures and their potential applications in catalytic and biological science [15–18]. Each arm of tripodal ligands can rotate freely around a N(apical)-C bond, and different components of pendants might exhibit a variety of biological functions [19–23]. The introduction of N-heterocyclic groups, such as imidazole, pyridine, pyrazole, and benzimidazole derivatives, is the common way to design and obtain the desired structures [24–30]. Moreover, imidazole or pyridine moieties play an important role in bioactive compounds and pharmacological interest of these polydentate ligands have already been established [31–33]. Taurine, the special amino acid containing sulfur, has important applications in medicine and biochemistry. A number of complexes with taurine-based ligands have various biological activities, such as antiviral, anticancer, and antibacterial [34, 35].

In this article, we report the syntheses and characterizations of two unsymmetrical tripodal ligands L1 and L2 (scheme 1), and their copper(II) complexes **1** and **2**. The binding activities of the complexes with calf thymus DNA (CT-DNA) were studied by UV–vis absorption spectroscopy, fluorescence spectroscopy, viscosity measurements, and DNA cleavage experiments. Cytotoxicities of **1** and **2** against eight cell lines (human hepatic cell line LO2, human breast cancer cell lines MCF-7 and MDA-MB-231, human non-small-cell lung cancer NCI-H460 and A549, human cervical cancer cell line HeLa, human hepatocellular carcinoma cell line HepG-2, and human gastric cancer cell line SGC-7901) were explored by MTT assay. The complexes have potential for antineoplastic effects toward HepG-2 cancer cells.

2. Experimental

2.1. *Materials and instrumentation*

2-(Chloromethyl)-l-methylimidazole hydrochloride was synthesized according to a previously reported procedure [36, 37], the other reagents and chemicals were purchased from commercial sources and used as received. Ethidium bromide (EB) and calf thymus DNA (CT-DNA) were purchased from Sigma. IR spectra were recorded as KBr disks on a Shimadzu IR-408 infrared spectrophotometer from 4000 to 600 cm^{-1}, and fluorescence spectral data were obtained on a MPF-4 fluorescence spectrophotometer at room

temperature. ^{1}H-NMR spectra were measured on a Bruker AVANCE III-400 spectrometer. The Gel Imaging and Documentation Digi Doc-It System were assessed by Labworks Imaging and Analysis Software (UVI, UK).

The tris(hydroxymethyl)aminomethane-HCl (Tris-HCl) buffer solution was prepared with triple-distilled water. All the experiments between the complexes and CT-DNA were carried out in Tris-HCl/NaCl buffer solution (pH 7.2, 5 mM Tris-HCl, 50 mM NaCl). CT-DNA stock solution was prepared by diluting DNA with Tris-HCl/NaCl buffer (pH 7.2) and kept at 4 °C for no longer than a week. The CT-DNA would be sufficiently free of protein when the ratio of its UV absorbance at 260 and 280 nm was in the range of 1.8–1.9; concentration of CT-DNA was determined by employing an extinction coefficient of 6600 M^{-1} cm^{-1} at 260 nm.

2.2. *Preparation of [Cu(L1)Cl_2]·3H_2O (1)*

2-(Chloromethyl)-l-methylimidazole hydrochloride (2.51 g, 15 mM) and taurine (0.6 g, 5 mM) were suspended in 25 mL distilled water. To this solution, N,N-diisopropylethylamine (1.94 g, 15 mM) and NaOH (1 g, 25 mM) both in 10 mL H_2O were slowly added in sequence during 1 h at room temperature. Then, the reaction mixture was refluxed and stirred continuously for 48 h in the dark. After cooling to room temperature, the resulting red solution was washed with $CHCl_3$ (25 mL) three times. The pH of the aqueous phase was adjusted to 6 by addition of 1 M HCl. The solvent was removed by evaporation, and then the resulting oil was dissolved in 90 mL anhydrous ethanol and filtered to remove insoluble substance. Solvent removal under vacuum afforded the crude product as a brown oil. The purification of L1 has not been successful so far even tried many times, so the crude product of L1 was directly used to react with Cu^{2+} by one-pot synthetic method as follows.

$CuCl_2·6H_2O$ (0.068 g, 0.4 mM) in aqueous solution (5 mL) was added dropwise to a methanol solution (15 mL) of L1 (0.136 g) with constant stirring. The mixture was stirred for 3 h and filtered. Diethyl ether was allowed to diffuse slowly into this solution at room temperature. Green single crystals of **1** were collected by filtration after several days. Yield: 37%. IR (KBr, cm^{-1}): 3465.0s, 2902.9m(br), 1649.9m, 1507.8m, 1425.4m, 1360.5m, 1174.8s, 1046.7s, 853.8w, 773.7m, 689.9m, 608.2m, 574.2m. Anal Calcd for $C_{17}H_{30}Cl_2CuN_7O_5S$ (%): C, 35.27; H, 5.22; N, 16.93. Found: C, 35.49; H, 5.26; N, 16.67.

2.3. *Preparation of bis(2-pyridylmethyl)amino]ethanesulfonic acid) (L2)*

L2 was prepared by a procedure similar to that given in the case of L1, but adding 2-chloromethylpyridine hydrochloride instead of 2-(chloromethyl)-l-methylimidazole hydrochloride to the reaction mixture. Yield: 59%. Main IR absorptions (KBr, cm^{-1}): 3562.1s, 3441.1s, 3046.7m, 2972.1m, 2936.0m, 2826.9m, 1632.4m, 1594.0s, 1570.3m, 1539.5w, 1436.5w, 1374.5w, 1297.2w, 1237.8s, 1198.0s, 1091.4w, 1043.4s, 997.8m, 914.2w, 807.7w, 768.9s, 740.5s, 665.3w, 620.0m, 600.1m, 524.8s. ^{1}H-NMR ($CDCl_3$): δ 2.92 (t, 2 H, CH_2), 3.49 (t, 2 H, CH_2), 3.94 (s, 4 H, CH_2), 7.31 (t, 4 H, CH-py), 7.73 (t, 2 H, CH-py), 8.49 (d, 2 H, CH-py). ^{13}C-NMR (D_2O): δ 156.75, 147.96, 138.24, 124.58, 123.21, 59.11, 49.30, 47.28.

2.4. *Preparation of [Cu(L2)Cl]·2H_2O (2)*

A methanol solution (12 mL) of L2 (0.132 g, 0.4 mM) was slowly added to an aqueous solution (4 mL) of $CuCl_2$•$6H_2O$ (0.068 g, 0.4 mM). The resulting blue reaction mixture was continuously stirred for 4 h at room temperature [38], filtered, and the filtrate left at room

temperature for crystallization. After four days, deep bluish green crystals suitable for X-ray analysis were obtained. Yield: 51%. IR (KBr, cm^{-1}): 3487.9m, 2924.3m, 1648.5m, 1609.9s, 1483.4m, 1447.7s, 1285.3s, 1221.2s, 1197.8s, 1163.2m, 1035.8s, 769.7s, 749.8w, 657.2w, 610.9w, 591.4 m. Anal Calcd for $C_{14}H_{20}ClCuN_3O_5S$ (%): C, 39.10; H, 4.57; N, 9.52. Found: C, 38.09; H, 4.86; N, 9.43.

2.5. *X-ray crystallography*

The diffraction data of **1** and **2** were determined by single-crystal X-ray experiments on a Bruker SMART 1000 CCD diffractometer equipped with graphite monochromated Mo-K_α radiation. Data collection and reduction were performed using SMART and SAINT software. An empirical absorption correction (SADABS) was applied to the raw intensities. The structure was solved by direct methods and refined by full-matrix least squares based on F^2 using the SHELXTL-97 program package. Hydrogens were included at geometrically calculated positions and refined using a riding model except those bonded to oxygen in water, which were located on a difference Fourier map. Experimental conditions for diffraction analysis, structural analysis, the correction method, and the crystal data are listed in table 1.

Table 1. Crystal data and structure refinements for **1** and **2**.

Complex	**1**	**2**
Empirical formula	$C_{17}H_{30}Cl_2CuN_7O_5S$	$C_{14}H_{20}ClCuN_3O_5S$
Formula weight	578.98	441.38
Temperature (K)	386(2)	113(2)
Wavelength (Å)	0.71073	0.71073
Crystal system	Monoclinic	Triclinic
Space group	*P*2(1)/*n*	*P-1*
a (Å)	8.252(3)	7.0594(14)
b (Å)	22.088(8)	11.199(2)
c (Å)	13.179(5)	11.962(2)
α (°)	90	104.81(3)
β (°)	102.379(5)	106.35(3)
γ (°)	90	95.15(3)
V (Å^3)	2346.2(16)	863.9(3)
Z	4	2
D_{Calcd} (g/cm^3)	1.639	1.697
Absorption coefficient (mm^{-1})	1.293	1.571
F(0 0 0)	1200	454
Crystal size (mm)	0.20 × 0.15 × 0.12	0.14 × 0.12 × 0.10
Theta range for date collection	1.83–25.15	2.24–25.01
Limiting indices	$-9 \le h \le 9$, $-26 \le k \le 26$, $-15 \le l \le 15$	$-8 \le h \le 7$, $-13 \le k \le 13$, $-14 \le l \le 11$
Reflections collected/unique	19,895/4201 [R_{int} = 0.0754]	5021/3036 [R_{int} = 0.0432]
Completeness to theta	25.15, 100.0%	25.01, 99.5%
Max. and min. transmission	0.8603 and 0.7821	0.8587 and 0.8101
Data/restraints/parameters	4201/0/307	3036/6/242
Goodness of fit on F^2	1.120	1.049
Final *R* indices [$I > 2\sigma(I)$]	R_1 = 0.0704, wR_1 = 0.1505	R_1 = 0.0386, wR_1 = 0.0982
R indices (all data)	R_1 = 0.0851, wR_2 = 0.1588	R_1 = 0.0456, wR_1 = 0.0995
Largest diff. peak (e Å^{-3})	1.208 and −1.238	0.715 and −1.050

2.6. *DNA binding and cleavage experiments*

Absorption titration experiments were performed by maintaining the concentration of the complex (100 μM) while gradually increasing the concentration of CT-DNA (0–150 μM); absorption was recorded after each addition of CT-DNA.

The competitive binding experiments of Cu(II) complexes treated with an EB-bound CT-DNA solution was determined by adding a certain amount of a solution of the complex step-by-step into the EB-DNA solution. The complex was added to CT-DNA solution treated with EB (4 μM EB and 80 μM CT-DNA). The influence of the addition of Cu(II) complexes to the EB-DNA complex has been obtained by recording the variation of fluorescence emission spectra with excitation at 510 nm and emission at 589 nm. Before the emission spectra were recorded, the complex-DNA solutions were incubated at room temperature for 5 min.

Viscosity measurements of 100 μM CT-DNA in Tris–HCl/NaCl buffer were performed using an Ubbelohde viscometer at 37 ± 0.1 °C in a thermostatic water bath. Flow time was measured with a digital stopwatch, and each sample was measured three times, and an average flow time was calculated.

Data are presented as $(\eta/\eta_0)^{1/3}$ *versus* binding ratio [Complex]/[DNA], where η and η_0 indicate the viscosity of DNA solutions in the presence and absence of complex, respectively. The relative viscosity was calculated according to the relation $\eta = (t - t_0)/t_0$, where t is the flow time of DNA solution in the presence or absence of complex and t_0 is the flow time of the buffer alone [39].

DNA cleavage experiments were done by agarose gel electrophoresis following the literature method [40, 41]. pUC19 DNA (0.05 μg μL^{-1}) in Tris buffer (pH 7.2, 50 mM Tris-HCl, 18 mM NaCl) was treated with varying concentrations of complexes and a fixed concentration of H_2O_2 (250 μM). The samples were incubated at 37 °C for 3 h and loading buffer was added. Then, the samples were electrophoresed for 30 min under 90 V on 1% agarose gel using Tris–boric acid–EDTA buffer. After electrophoresis, bands were visualized by UV light and photographed by the Gel Imaging and Documentation Digi Doc-It System. Cleavage mechanistic investigation of pUC19 DNA was measured in the presence of standard radical scavengers and reaction inhibitors, including DMSO, NaN_3, SOD, EDTA, KI, and L-histidine, added to pUC19 DNA and complex. Cleavage experiments were initiated by addition of complex and quenched with 4 μL of loading buffer. Further analysis was carried out by the above standard method.

2.7. *Cytotoxicity assay*

2.7.1. Cell culture. MCF-7, MDA-MB-231, NCI-H460, A549, HeLa, and HepG-2 cells were purchased from the American Type Culture Collection (Rockville, MD, USA). SGC-7901 and LO2 cells were obtained from the China Center for Type Culture Collection (CCTCC). They were grown in Dulbecco's modified Eagle's Medium (DMEM), which was supplemented with 10% FBS, 100 U mL^{-1} penicillin, and 100 μg mL^{-1} streptomycin. Cells were maintained in a humidified atmosphere containing 95% air and 5% CO_2 at 37 °C.

2.7.2. MTT assay. Cell viability was examined by MTT assay, which is a colorimetric assay based on conversion of the yellow tetrazolium salt MTT to purple formazan crystals by metabolically active cells [42]. Varied kinds of cells (1×10^4 per well) plated in 96-well

plates were incubated at 37 °C in a 5% CO_2 humidified atmosphere for 24 h; the cells were subsequently treated with different concentrations of **1**, **2,** and cisplatin ranging from 0 to 40 μM for 48 h. Then, 10 μL MTT (5 mg mL^{-1}) in phosphate buffered saline (PBS, pH 7.4) was added to each well. After 4 h, the supernatant was removed and 100 μL DMSO was added to dissolve the MTT formazan precipitate. The absorbance of samples was read at 570 nm using an enzyme-linked immunosorbent assay (ELISA) reader. The experiments were carried out in triplicate and IC_{50} values were calculated from plots of cell viability against the logarithm of drug concentration added.

3. Results and discussion

3.1. *IR spectra*

In IR spectra of L2, **1** and **2**, strong bands from 3600 to 3400 cm^{-1} can be ascribed to *ν*(O–H), due to hydroxyl group for L2 and lattice water for **1** and **2**. For L2, the medium–strong bonds at 1632 and 1594 cm^{-1} are assigned to *ν*(C=N), shifted to higher frequencies upon complexation (1648, 1610 cm^{-1} for **2**), indicating coordination of the heterocyclic nitrogens [43]. For **1**, *ν*(C=N) is at 1650 cm^{-1}. Strong absorptions are observed at 1238, 1198, and 1043 cm^{-1} for L2, typical for sulfonate [44, 45]. For **2**, the corresponding absorptions shift to 1285, 1221, and 1198 cm^{-1}, suggesting that oxygen of sulfonate coordinates [46]. For **1**, strong absorptions for sulfonate are observed at 1175 and 1047 cm^{-1}.

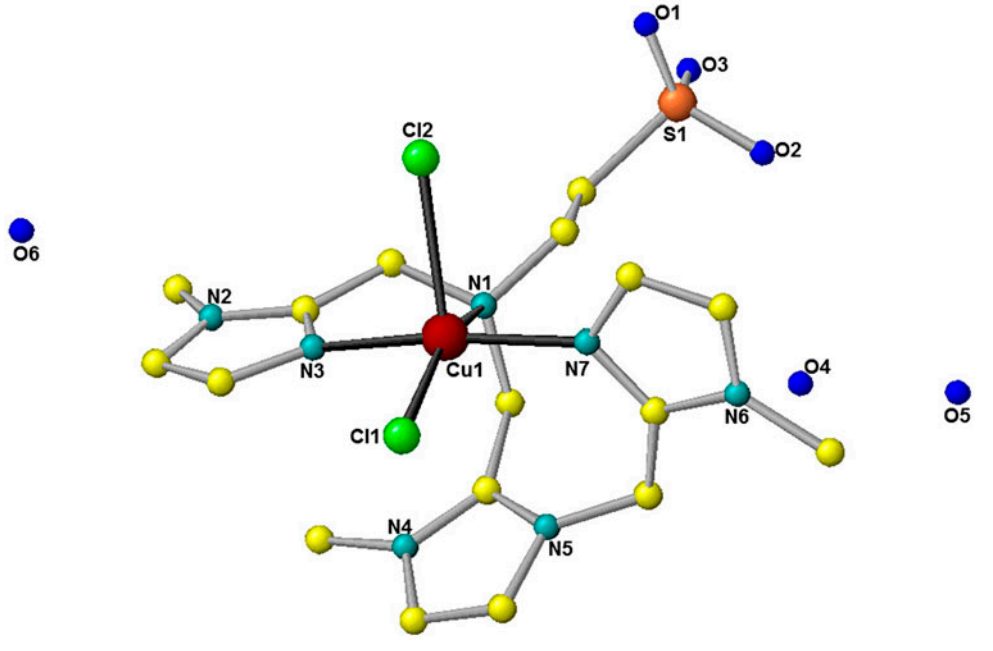

Figure 1. A perspective view of **1**. Hydrogens are omitted for clarity.

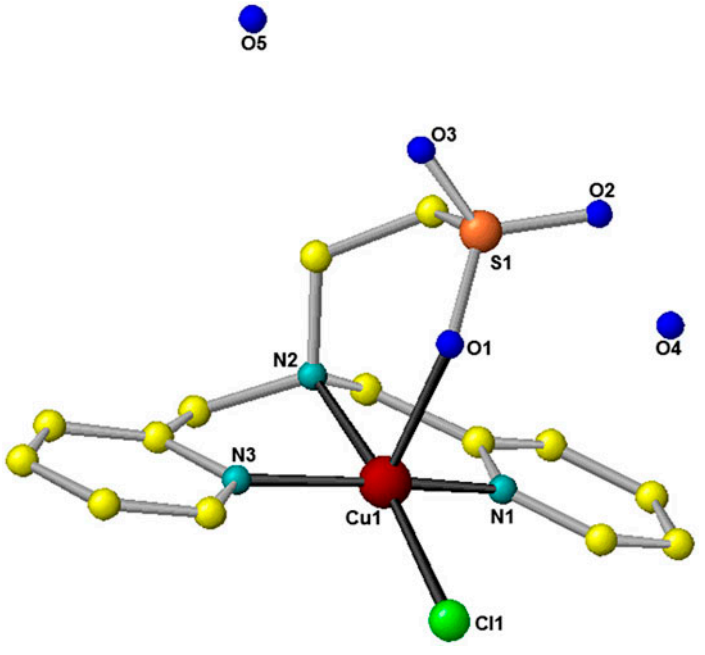

Figure 2. A perspective view of **2**. Hydrogens are omitted for clarity.

Table 2. Selected bond lengths (Å) and angles (°) for **1** and **2**.

1		**2**	
Cu1–N1	2.232(5)	Cu1–N1	1.981(3)
Cu1–N7	1.974(5)	Cu1–N3	1.979(3)
Cu1–Cl2	2.5086(17)	Cu1–O1	2.270(3)
Cu1–N3	1.964(5)	Cu1–N2	2.055(3)
Cu1–Cl1	2.3034(16)	Cu1–Cl1	2.2457(13)
N3–Cu1–N7	167.94(19)	N3–Cu1–N1	160.92(12)
N7–Cu1–N1	90.75(17)	N1–Cu1–N2	83.46(11)
N7–Cu1–Cl1	92.12(13)	N1–Cu1–Cl1	96.44(9)
N3–Cu1–Cl2	92.84(14)	N3–Cu1–O1	93.20(11)
N1–Cu1–Cl2	94.56(12)	N2–Cu1–O1	93.52(10)
N3–Cu1–N1	80.24(18)	N3–Cu1–N2	82.94(11)
N3–Cu1–Cl1	92.77(14)	N3–Cu1–Cl1	94.83(9)
N1–Cu1–Cl1	155.07(12)	N2–Cu1–Cl1	170.70(9)
N7–Cu1–Cl2	95.87(14)	N1–Cu1–O1	100.95(11)
Cl1–Cu1–Cl2	109.76(5)	Cl1–Cu1–O1	95.63(7)

3.2. *Description of crystal structure*

The perspective view of $[Cu(L1)Cl_2]\cdot 3H_2O$ (**1**) and $[Cu(L2)Cl]\cdot 2H_2O$ (**2**) is shown in figures 1 and 2. Selected bond lengths and angles are listed in table 2. Complex **1** comprises one neutral mononuclear $[Cu(L1)Cl_2]$ and three lattice waters. For L1, besides two N-methyl-imidazolylmethyl pendent arms linked directly to apical N, there is an extra N-methyl-imidazolylmethyl group linking to one of the arms, resulting in an unsymmetrical

tripodal L1. Due to the high activity of 2-(chloromethyl)-N-methylimidazole under basic conditions, the extra N-methyl-imidazolylmethyl group could link with the imidazolyl nitrogen of the imidazole ring by nucleophilic substitution. In **1**, Cu is coordinated to three nitrogens (N1, N3, and N7) from L1 and two chlorides (Cl1 and Cl2). The coordination geometry around Cu(II) could be best described as a distorted square pyramid with a value of 0.2 for τ parameter [47, 48], $\tau = (\alpha - \beta)/60$, [where α = N(3)–Cu(1)–N(7) = 167.89(19)° and β = N(1)–Cu(1)–Cl(1) = 155.08(13)°]. The value of τ describes the degree of distortion of the metal ion in five-coordinate complexes, that $\tau = 1$ for an ideal trigonal-bipyramid and $\tau = 0$ for an ideal square pyramid [49, 50]. Three nitrogens (N1, N3, and N7) and one chloride (Cl1) occupy the equatorial plane, and chloride (Cl2) occupies the apical position. Due to the Jahn–Teller effect for d^9 configuration of Cu(II) in a square-pyramidal environment, the axial Cu–Cl2 distance (2.5086(17) Å) is longer than the in plane Cu–Cl1 distance (2.3034(16) Å) [51]. The $Cu–N_{imidazole}$ bond (Cu–N3, 1.964(5) Å) is shorter than the $Cu–N_{amine}$ bond (Cu–N1, 2.232(5) Å), which is expected for sp^2 and sp^3 hybridizations, respectively [52]. As shown in figure 1, L1 is an unsymmetrical tripodal ligand with three different pendant arms including N-methyl-imidazolylmethyl, N-methyl-N′-(N-methyl-imidazolylmethyl) imidazolylmethyl, and sulfonic acid, thus giving the corresponding unsymmetrical Cu(II) complex, in which one $Cu–N_{imidazole}$ bond (Cu–N7, 1.974(5) Å) is a little longer than the other $Cu–N_{imidazole}$ bond (Cu–N3) arising from steric hindrance of adjacent methylimidazole substituent [53].

As shown in figure 2, **2** comprises one mononuclear Cu(II) unit and two lattice waters. In the mononuclear unit, copper is coordinated by three nitrogens and one oxygen from L2 and one chloride. The value (0.16) of the trigonality index [$\tau = (\alpha - \beta)/60$, where α = N(3)–Cu(1)–N(1) = 160.92(12)° and β = N(2)–Cu(1)–Cl(1) = 170.70(9)°] reveals that copper(II) in **2** is a distorted square-pyramidal geometry. In this geometry, three nitrogens (N1, N2, and N3) and one chloride (Cl1) occupy the equatorial plane and one oxygen (O1) occupies the apical position. The Cu–N (Cu–N1, 1.981(3) Å; Cu–N2, 2.055(3) Å; Cu–N3, 1.979(3) Å) and the Cu–Cl(1) (2.2457(13) Å) bond lengths are similar to those in **1**. Thus, the apical Cu–O1 bond (2.270(3) Å) is longer than all the bonds (1.979(3)–2.2457(13) Å) in the basal plane, which is also due to the Jahn–Teller effect [54].

3.3. *DNA binding and cleavage activities*

3.3.1. UV–vis absorption spectroscopy. UV–vis absorption spectroscopy is a common way to investigate the interactions of complexes with DNA. The absorption spectra of **1** and **2** in the absence and presence of CT-DNA at different concentrations are given in figure 3. The maximal absorption peaks at 226 and 255 nm for **1** and **2**, arising from intraligand π–π^* transitions, displayed hypochromism of 13.69 and 13.49%, respectively, upon increasing amounts of CT-DNA. The binding constant K_b was determined using the following equation [55]:

$$[\mathrm{DNA}]/(\varepsilon_a - \varepsilon_f) = [\mathrm{DNA}]/(\varepsilon_b - \varepsilon_f) + 1/K_b(\varepsilon_b - \varepsilon_f) \quad (1)$$

where [DNA] is the concentration of DNA, ε_a, ε_f, and ε_b correspond to the extinction coefficient of the complex at a given DNA concentration, the extinction coefficient of the complex free in solution, and the extinction coefficient of the complex when fully bound to DNA, respectively. From the observed spectrometric changes, the values of

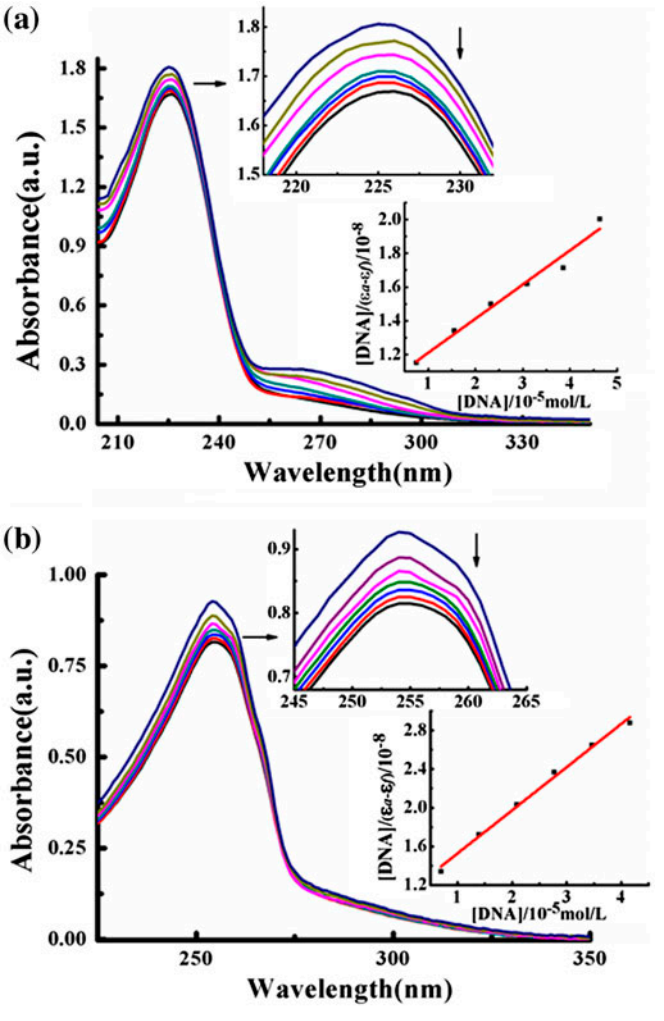

Figure 3. Absorption spectra of **1** (100 μM) (a) and **2** (72 μM) (b) in the absence and presence of increasing amounts of CT-DNA at room temperature in Tris–HCl/NaCl buffer (pH 7.2). Inset: (1) an expansion of the lambda max region; (2) plot of $[DNA]/(\varepsilon_a - \varepsilon_f)$ *vs.* [DNA] for absorption titration of CT-DNA with complex.

the intrinsic binding constants K_b ($2.46 \times 10^4\ M^{-1}$ for **1** and $1.01 \times 10^4\ M^{-1}$ for **2**) were determined by regression analysis using equation 1. The K_b values of **1** and **2** are lower than observed for a classical intercalator (e.g. ethidium bromide (EB), $\sim 10^6\ M^{-1}$) [56] and close to those of complexes with similar aromatic planar structure, such as $[Cu_2(pdmaeox)(bpy)(H_2O)](pic)\cdot H_2O$ ($K_b = 3.39 \times 10^4\ M^{-1}$) [$H_3$pdmaeox = N-phenolato-N′-[2-(dimethylamino)ethyl]oxamide, Hpic = 2,4,6-trinitrophenol, bpy = 2,2′-bipyridine] [57], and $[Cu_2(heap)(H_2O)_2](pic)_2\cdot 2H_2O$ ($K_b = 2.67 \times 10^4\ M^{-1}$) [heap = N,N′-bis(N-hydroxyethylaminopropyl)oxamide, Hpic = 2,4,6-trinitrophenol] [58]. However, they are larger than some mono- and bi-copper(II) complexes containing such aromatic ligands with additional substituent group, such as {Cu_2[2-((2-hydroxybenzylidene)

amino)-4-(methylthio)butanoic]$_2$(H_2O)} ($K_b = 4.91 \times 10^3$ M^{-1}), {[Cu_2(2-((2-hydroxybenzyl)amino)-4-(methylthio)butanoic acid)$_2$(H_2O)]·H_2O} ($K_b = 8.75 \times 10^3$ M^{-1}) [59], [Cu_2(μ-Cl)$_2$(O-2-butoxyethylpyridine-2-carboximidate)$_2Cl_2$] ($K_b = 1.524 \times 10^3$ M^{-1}) [60], and [Cu_2(bpdc)$_2H_2O$]·$2H_2O$ ($K_b = 2.17 \times 10^3$ M^{-1}) (H_2bpdc = 2,2′-bipyridine-6,6′-dicarboxylic acid) [61]. The K_b value observed for the present complexes implies that neither **1** nor **2** can intercalate very strongly or deeply between the DNA base pairs. We propose that the weak hypochromism observed in UV–vis spectra probably arises from the partial intercalation of **1** and **2** into CT-DNA, in which the small planarity of imidazolyl/pyridyl ring and the steric hindrance of the other two arms of tripodal ligand in **1** and **2** might reduce the inserting degree of complex to DNA. In addition, methyl, as an electron donating group, will increase the electron density on the intercalating ligands, hence reinforcing the repulsion between the complex and DNA with the negatively charged phosphate backbone, and consequently destabilize the DNA-complex system, causing a decrease in the DNA-binding affinity [62].

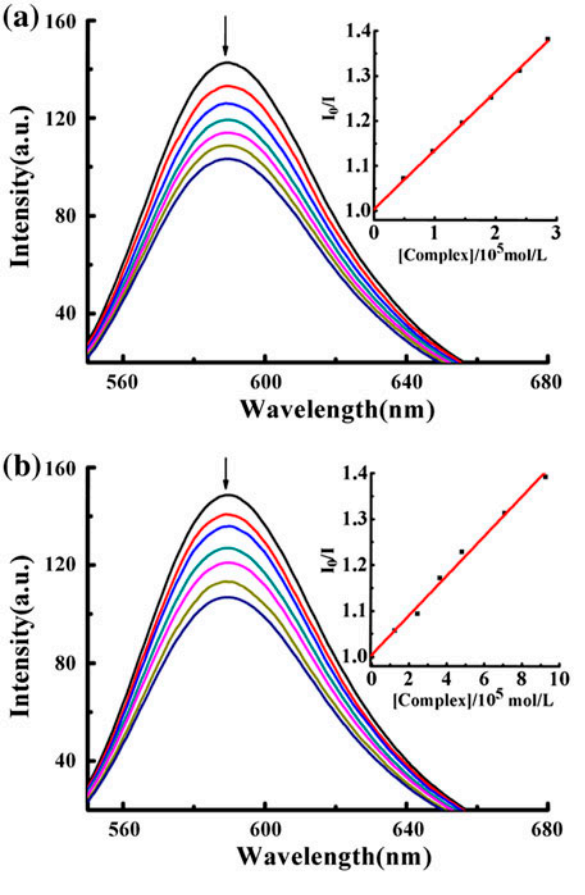

Figure 4. Fluorescence quenching curves of EB bound to DNA by **1** ([complex] = 0–2.85×10^{-5} M) (a) and **2** ([complex] = 0–9.25×10^{-5} M) (b). The arrow shows the intensity changes on increasing the complex concentration. Inset: plot of I_0/I *vs.* [complex], λ_{ex} = 510 nm.

3.3.2. Fluorescence spectroscopy studies. Fluorescence measurements were performed to clarify the complexes bind to DNA via intercalation using a MPF-4 fluorescence spectrophotometer. No luminescence could be observed for **1** and **2** at room temperature in aqueous solution, and therefore, the binding of copper(II) complexes to DNA is evaluated by the fluorescence emission intensity of EB-DNA solution as a probe. The competitive binding experiments were carried out with an EB-bound CT-DNA solution in Tris–HCl/NaCl buffer. As shown in figure 4, fluorescence intensities at 589 nm (510 nm excitation) were measured after addition of different concentrations of **1** and **2**, which suggested the complex could compete with EB to bind to DNA with similar intercalating fashion.

As shown in figure 4, the fluorescence quenching curves showed that the quenching of EB-DNA system by **1** and **2** is both in agreement with the classical Stern–Volmer equation [62]: $I_0/I = 1 + K[Q]$. From the equation $K_{EB}[EB] = K_{app}[complex]$ (where [complex] is the value at a 50% reduction of the fluorescence intensity of EB, $K_{EB} = 1.0 \times 10^7\ M^{-1}$, and [EB] = 4 μM), the value of apparent binding constants (K_{app}) was calculated to be 3.12×10^5 for **1** and 1.03×10^5 for **2**, which were less than the classical binding constant ($K_{EB} = 10^7\ M^{-1}$ reported by Cory *et al.* [63, 64]). Our results are consistent with some earlier reports on quenching fluorescence of EB-DNA for Cu complexes with similar K_{app} value [65–68], suggesting that the interaction of **1** and **2** with DNA is a moderate intercalative mode. The modes and affinities of DNA binding of these copper(II) complexes mainly depend on the nature of the ligands.

3.3.3. Viscosity measurements. In order to examine the intercalative mode of binding between the complexes and DNA, viscosity studies were also carried out. A classical intercalative mode will cause a significant increase in viscosity of DNA solution due to enhancing of separation of base pairs at intercalation site and the unwinding of DNA helix will lead to an overall increase for the DNA length [69]. By contrast, groove binding and electrostatic interactions only cause slight or no changes of viscosity [70]. The viscosity

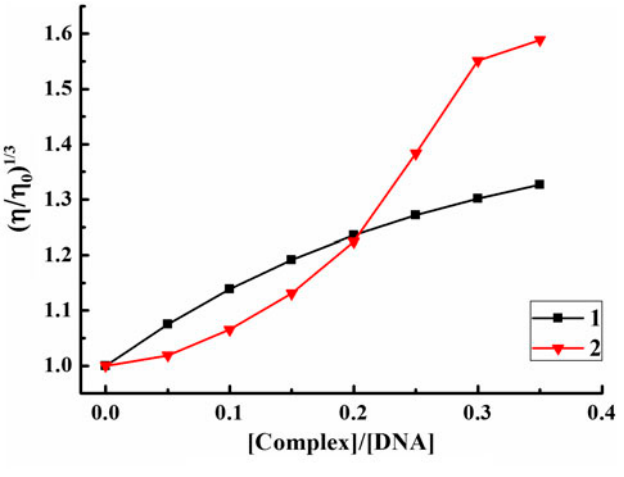

Figure 5. Effects of increasing amounts of **1** and **2** on the relative viscosity of CT-DNA. ([complex] = 0–0.875 × 10^{-5} M).

experiments were carried out on CT-DNA by varying the concentration of the complexes, and the corresponding data are illustrated in figure 5. Complexes **1** and **2** show different binding behavior with changes in concentration. At a low complex concentration ([complex]/[DNA] = 0.0–0.2), the specific viscosity of CT-DNA obviously increased, and the order of relative viscosity of the CT-DNA is **1** > **2**, indicating the binding ability of **1** is higher than **2**. However, the viscosity of the DNA was found to slightly increase for **1** at a higher concentration ([complex]/[DNA] > 0.2), but rapidly increased for **2**, and the ability of the complexes to increase the viscosity of DNA varies as: **2** > **1**. The viscosity experiments were carried out in triplicate and the data were reproducible, but the exact explanation for this difference induced by **1** and **2** is unknown.

Upon increasing the concentration of **1** and **2**, the specific viscosity of CT-DNA obviously increased. Such behavior is consistent with other intercalators (i.e. EB) and further confirmed that both **1** and **2** could bind to DNA by intercalation [71–73].

3.3.4. DNA cleavage activities. The ability of the complexes to cause DNA cleavage in the presence of H_2O_2 has been investigated by gel electrophoresis using plasmid pUC19 DNA in Tris–HCl/NaCl buffer solution (pH 7.2). When the original supercoiled form (Form I) of plasmid DNA is nicked, an open circular relaxed form (Form II) can be found in the system. When conducted by electrophoresis, the compact Form I migrates relatively faster while the nicked Form II migrates slowly. Control experiments using only H_2O_2 (250 μM) and no obvious DNA cleavage were observed (lane 2). With increased concentration of complexes, Form I plasmid DNA was gradually converted into Form II. The results indicate that the copper complexes can cleave plasmid DNA in the presence of H_2O_2.

Depending on the number of electrons transferred from the complex to O_2, several possible intermediates such as hydroxyl radical (**.**OH), singlet oxygen ($^1O_2$), superoxide anion (O_2^-), and hydrogen peroxide (H_2O_2) could be involved in copper-mediated oxidative DNA cleavage. To elucidate the cleavage mechanism of pUC19 plasmid DNA induced by **1** and

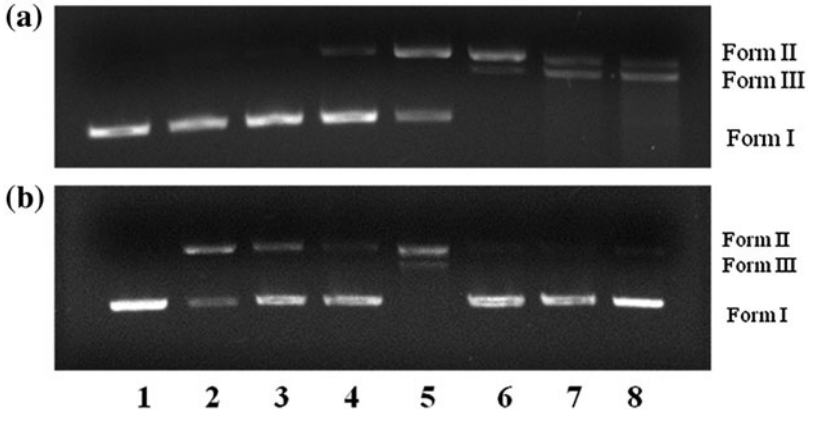

Figure 6. Gel electrophoresis diagram of **1**. (a) Lane 1: DNA control; Lane 2: DNA + H_2O_2 (250 μM), Lanes 3–8: DNA + H_2O_2 (250 μM) + **1** (2.08, 4.17, 10.42, 20.83, 41.67, 83.33 μM); (b) Lane 1: DNA control; lane 2: DNA + **1** (10.42 μM) + H_2O_2 (250 μM); lane 3: DNA + **1** + H_2O_2 + DMSO (20 mM); lane 4: DNA + **1** + H_2O_2 + NaN_3 (20 mM); lane 5: DNA + **1** + H_2O_2 + SOD (6 units); lane 6: DNA + **1** + H_2O_2 + EDTA (5 mM); lane 7: DNA + **1** + H_2O_2 + KI (20 mM); lane 8: DNA + **1** + H_2O_2 + L-histidine (20 mM).

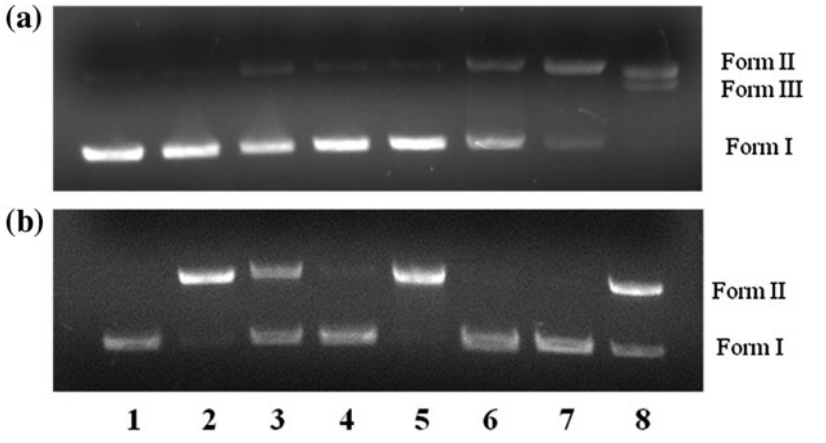

Figure 7. Gel electrophoresis diagram of **2**. (a) Lane 1: DNA control; Lane 2: DNA + H_2O_2 (250 μM), Lanes 3–8: DNA + H_2O_2 (250 μM) + **2** (2.08, 4.17, 10.42, 20.83, 41.67, 83.33 μM); (b) Lane 1: DNA control; lane 2: DNA + **2** (20.83 μM) + H_2O_2 (250 μM); lane 3: DNA + **2** + H_2O_2 + DMSO (20 mM); lane 4: DNA + **2** + H_2O_2 + NaN_3 (20 mM); lane 5: DNA + **2** + H_2O_2 + SOD (6 units); lane 6: DNA + **2** + H_2O_2 + EDTA (5 mM); lane 7: DNA + **2** + H_2O_2 + KI (20 mM); lane 8: DNA + **2** + H_2O_2 + L-histidine (20 mM).

2, we investigated DNA cleavage in the presence of hydroxyl radical scavenger (DMSO), singlet oxygen quenchers (NaN_3, L-histidine), superoxide scavenger (SOD), hydrogen peroxide scavenger (KI), and chelating agent (EDTA) under the same conditions. As demonstrated in figures 6(b) and 7(b), no obvious inhibitions could be observed in the presence of DMSO (lane 3) and SOD (lane 5), indicating noninvolvement of hydroxyl radical and superoxide radical in the cleavage reaction. The Cu^{II}-specific chelating agent, EDTA (lane 6), efficiently inhibited DNA cleavage, suggesting both **1** and **2** play crucial roles in the cleavage. Potassium iodide (lane 7) significantly diminished the nuclease activity of **1** and **2**, indicative of hydrogen peroxide in the cleavage process. Addition of singlet oxygen scavengers like NaN_3 (lane 4) and L-histidine (lane 8) showed inhibition of nuclease, suggesting that $^1O_2$ or any other singlet oxygen-like entity may participate in the DNA

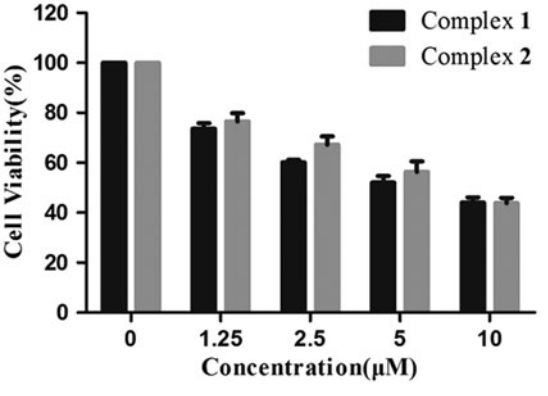

Figure 8. Cell viability of HepG-2 cells after treatment with **1** and **2** for 48 h by MTT assay.

Table 3. IC_{50} values of **1**, **2**, cisplatin, and similar mono-copper(II) complexes against HepG-2 cell line.

Complex	IC_{50} (μM)	References
1	6.2 ± 2.5	This work
2	7.1 ± 1.9	This work
Cisplatin	18.9 ± 4.3	This work
[CuLCl]ClO_4 [L = N,N-bis(quinolin-2-ylmethyl)quinolin-8-amine]	5.957	[41]
[Cu^{II}(ClQP)(NO_3)(H_2O)] (HClQP = 4-chloro-2(quinolin-8-yliminomethyl)-phenol)	6.5 ± 0.3	[76]
[Cu(Am4M)(OAc)]·H_2O ([HAm4M = (Z)-2-(amino(pyridin-2-yl)methylene)-N-methylhydrazinecarbothioamide])	11.2 ± 0.9	[77]

strand scission [74, 75]. The results suggest that both **1** and **2** cleave DNA via oxidative cleavage.

3.4. *Cytotoxicity evaluation*

The cytotoxicity of **1**, **2**, and cisplatin against seven different kinds of cancer cell lines and one normal cell line LO2 were detected by MTT assay. Cells were incubated with complexes at different concentrations for 48 h. Among seven tested cancer cell lines, HepG-2 (IC_{50} values < 10 μM) was most sensitive to **1** and **2**, suggesting that these complexes have cytotoxic selectiveness in cell types. Dose-response curves of complexes against HepG-2 cells are shown in figure 8. The results indicated that **1** and **2** were cytotoxic to HepG-2 cells and inhibit the growth of cells in a dose-dependent manner. The IC_{50} values at 48 h were 6 ± 2 μM for **1** and 7 ± 2 μM for **2**, while 18 ± 4 μM for cisplatin. Compared to cisplatin, **1** and **2** showed twofold cytotoxicity, which is consistent with some similar mono-copper(II) complexes on HepG-2 cell lines [76, 77] (listed in table 3). The redox properties of copper ion may be important, owing to its variable valence. In the presence of Cu(II), antioxidants could generate ROS to damage DNA that might be an important pathway in cell apoptosis. These results show that both **1** and **2** have the potential as effective chemotherapeutic agents especially toward HepG-2 cell lines (scheme 1).

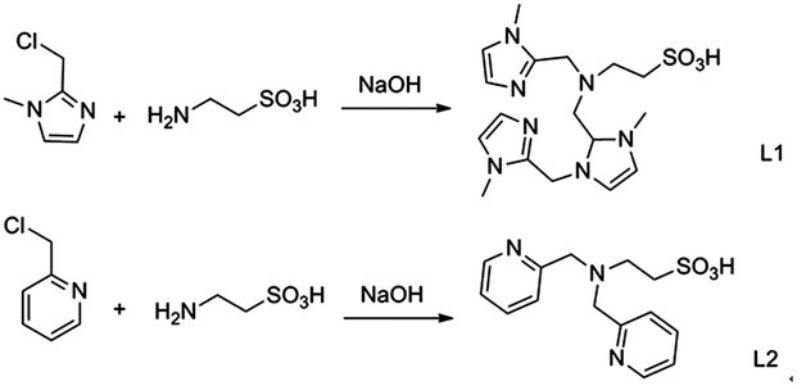

Scheme 1. The reaction pathways of L1 and L2.

Interestingly, the IC_{50} values of **1** and **2** in human hepatocellular carcinoma cell line HepG-2 were lower than human normal hepatic cell lines LO2 (>10 μM). However, there was no significant difference on cytotoxicity between **1** and **2**. The present study suggested that **1** and **2** may be antitumor agents with high-efficiency and low-toxicity on HepG-2 breast cancer cells.

4. Conclusion

Two mononuclear copper(II) complexes with new unsymmetrical tripodal ligands have been synthesized and characterized. Partial intercalation between the complexes and CT-DNA has been confirmed by various spectroscopic and viscosity measurements. Compared to copper complexes reported in the literature, **1** and **2** exhibited a moderate binding affinity with DNA, probably owing to the planarity of imidazolyl or pyridyl ring and the steric hindrance from tripodal ligands. Both **1** and **2** displayed effective oxidative DNA cleavage activity in the presence of H_2O_2. Moreover, they both showed significant cytotoxic activity toward the HepG-2 cell lines, and the IC_{50} values of **1** and **2** are considerably lower than the clinically used cisplatin under *in vitro* conditions. The results from our present study suggest that **1** and **2** deserve further investigation as potential antitumor drugs.

Supplementary materials

Crystallographic data for the structure reported in this article have been deposited with the Cambridge Crystallographic Data Center, CCDC No. 994176 and 1008460. Copies of this information may be obtained free of charge from the CCDC (E-mail: deposit@ccdc.cam.ac.uk or www: http://www.ccdc.cam.ac.uk).

Disclosure statement

No potential conflict of interest was reported by the authors.

Funding

This work was supported by the National Natural Science Foundation of China [grant number 21371135]; the Key Program of Tianjin Municipal Natural Science Foundation [grant number 13JCZDJC28200].

References

[1] N. Shahabadi, M. Falsafi, N.H. Moghadam. *J. Photochem. Photobiol., B*, **122**, 45 (2013).
[2] L.M. Chen, J. Liu, J.C. Chen, S. Shi. *J. Mol. Struct.*, **881**, 156 (2008).
[3] J.K. Barton, E.D. Olmon, P.A. Sontz. *Coord. Chem. Rev.*, **255**, 619 (2011).
[4] H.K. Liu, P.J. Sadler. *Acc. Chem. Res.*, **44**, 349 (2011).
[5] M. Demeunynck, C. Bailly, W.D. Wilson. *Small Molecule DNA and RNA Binders: From Synthesis to Nucleic Acid Complexes*, Wiley-VCH, Weinheim (2004).
[6] K.R. Chaurasiya, T. Paramanathan, M.J. McCauley, M.C. Williams. *Phys. Life Rev.*, **7**, 299 (2010).
[7] Z. Wu, Q. Liu, X. Liang, X. Yang, N. Wang, X. Wang, H. Sun, Y. Lu, Z. Guo. *J. Biol. Inorg. Chem.*, **14**, 1313 (2009).

[8] E.C. Bielefeld, C. Tanaka, G. Chen, D. Coling, M. Li, D. Henderson, A.R. Fetoni. *Anti-Cancer Drugs*, **24**, 43 (2013).
[9] K. Garbutcheon-Singh, M.P. Grant, B.W. Harper, A.M. Krause-Heuer, M. Manohar, N. Orkey, J.R. Aldrich-Wright. *Curr. Top. Med. Chem.*, **11**, 521 (2011).
[10] D. García Sar, M. Montes-Bayón, E. Blanco-González, A. Sanz-Medel. *TrAC, Trends Anal. Chem.*, **29**, 1390 (2010).
[11] M.J. Li, T.Y. Lan, Z.S. Lin, C.Q. Yi, G.N. Chen. *J. Biol. Inorg. Chem.*, **18**, 993 (2013).
[12] J. Easmon, G. Pürstinger, G. Heinisch, T. Roth, H.H. Fiebig, W. Holzer, W. Jäger, M. Jenny, J. Hofmann. *J. Med. Chem.*, **44**, 2164 (2001).
[13] Z.Y. Ma, X. Qiao, C.Z. Xie, J. Shao, J.Y. Xu, Z.Y. Qiang, J.S. Lou. *J. Inorg. Biochem.*, **117**, 1 (2012).
[14] C.Z. Xie, M.M. Sun, S.H. Li, X.T. Zhang, X. Qiao, Y. Ouyang, J.Y. Xu. *J. Coord. Chem.*, **66**, 3891 (2013).
[15] T. Nebe, J.Y. Xu, A. Beitat, C. Würtele, O. Walter, M. Serafin, S. Schindler. *Inorg. Chim. Acta*, **363**, 2965 (2010).
[16] S. Foxon, J.Y. Xu, S. Turba, M. Leibold, F. Hampel, F.W. Heinemann, O. Walter, C. Würtele, M. Holthausen, S. Schindler. *Eur. J. Inorg. Chem.*, **2007**, 429 (2007).
[17] J.Y. Xu, J. Astner, O. Walter, F.W. Heinemann, S. Schindler, M. Merkel, B. Krebs. *Eur. J. Inorg. Chem.*, **2006**, 1601 (2006).
[18] (a) H.L. Wu, J.G. Liu, P. Liu, W.B. Lv, B. Qi, X.K. Ma. *J. Coord. Chem.*, **61**, 1027 (2008); (b) H.L. Wu, X. Huang, J. Yuan, K. Li, J. Ding, R. Yun, W. Dong, X. Fan. *J. Coord. Chem.*, **62**, 3446 (2009).
[19] S.K. Sahoo, M. Baral, R.K. Bera, B.K. Kanungo. *J. Solution Chem.*, **40**, 1187 (2011).
[20] A.M. Pujol, C. Gateau, C. Lebrun, P. Delangle. *Chem. Eur. J.*, **17**, 4418 (2011).
[21] Q. Wang, K. Tang, X. Jin, X. Huang, W. Liu, X. Yao, Y. Tang. *Dalton Trans.*, **41**, 3431 (2012).
[22] M. Hirotsu, K. Kawamoto, R. Tanaka, Y. Nagai, K. Ueno, Y. Teki, I. Kinoshita. *Dalton Trans.*, **42**, 12220 (2013).
[23] S. Chakrabarty, P. Sarkhel, R. Poddar. *J. Coord. Chem.*, **61**, 3260 (2008).
[24] P. Torres-García, E. VIÑUelas-Zahínos, F. Luna-Giles, A. Bernalte-García. *J. Coord. Chem.*, **65**, 3556 (2012).
[25] T. Kurc, V.A. Veneta, T.T. Ilona, M. Duczmal. *J. Mol. Struct.*, **134–142**, 1054 (2013).
[26] A. Barattucci, M.R. Plutino, C. Faggi, P. Bonaccorsi, L. Monsù Scolaro, M.C. Aversa. *Eur. J. Inorg. Chem.*, **2013**, 3412 (2013).
[27] X.Y. Xu, J. Gao, M.Y. Wang, W.X. Ma, H.B. Song, K.P. Wainwright. *J. Coord. Chem.*, **58**, 669 (2005).
[28] J.R. Cubanski, S.A. Cameron, J.D. Crowley, A.G. Blackman. *Dalton Trans.*, **42**, 2174 (2013).
[29] Y.Y. Deng, D. Zhang, X.Q. Duan, X.S. Shen, F.Q. Liu. *J. Chem. Crystallogr.*, **44**, 185 (2014).
[30] K.J. Oberhausen, R.J. O'brien, J.F. Richardson, R.M. Buchanan. *Inorg. Chim. Acta*, **173**, 145 (1990).
[31] M. Pascaly, M. Duda, A. Rompel, B.H. Sift, W. Meyer-Klaucke, B. Krebs. *Inorg. Chim. Acta*, **291**, 289 (1999).
[32] V.M. Manikandamathavan, B. Unni Nair. *Eur. J. Med. Chem.*, **68**, 244 (2013).
[33] M. Li, L.L. Kong, Y. Gou, F. Yang, H. Liang. *Spectrochim. Acta, Part A*, **128**, 686 (2014).
[34] Y.M. Jiang, S.H. Zhang, Q. Xu, Y. Xiao. *Acta Chim. Sinica*, **61**, 573 (2003).
[35] L.Z. Li, Q. Guo, J.F. Dong, T. Xu, J.H. Li. *J. Photochem. Photobiol., B*, **125**, 56 (2013).
[36] N. Wei, N.N. Murthy, Z. Tyeklar, K.D. Karlin. *Inorg. Chem.*, **33**, 1177 (1994).
[37] C. Liao, X. Zhu, X.G. Sun, S. Dai. *Tetrahedron Lett.*, **52**, 5308 (2011).
[38] C.Y. Gao, X. Qiao, Z.Y. Ma, Z.G. Wang, J. Lu, J.L. Tian, J.Y. Xu, S.P. Yan. *Dalton Trans.*, **41**, 12220 (2012).
[39] S. Thalamuthu, B. Annaraj, S. Vasudevan, S. Sengupta, M.A. Neelakantan. *J. Coord. Chem.*, **66**, 1805 (2013).
[40] F. Xue, C.Z. Xie, Y.W. Zhang, Z. Qiao, X. Qiao, J.Y. Xu, S.P. Yan. *J. Inorg. Biochem.*, **115**, 78 (2012).
[41] J. Lu, J.L. Li, Q. Sun, L. Jiang, W. Gu, X. Liu, J.L. Tian, S.P. Yan. *Spectrochim. Acta, Part A*, **130**, 390 (2014).
[42] A. Ghadersohi, D. Pan, Z. Fayazi, D.G. Hicks, J.S. Winston, F.Z. Li. *Breast Cancer Res. Treat.*, **102**, 19 (2007).
[43] P.R. Reddy, A. Shilpa, N. Raju, P. Raghavaiah. *J. Inorg. Biochem.*, **105**, 1603 (2011).
[44] Z.H. El-Wahab, M.M. Mashaly, A.A. Salman, B.A. El-Shetary, A.A. Faheim. *Spectrochim. Acta, Part A*, **60**, 2861 (2004).
[45] Q.J. Zhou, X.J. Yao, L.F. Hao, Y. Ouyang, J.Y. Xu, C.Z. Xie, J.S. Lou. *Z. Anorg. Allg. Chem.*, **636**, 2487 (2010).
[46] K. Nakamoto. *Infrared Spectra and Raman Spectra of Inorganic and Coordination Compounds*, Wiley, New York (1986).
[47] Z.D. Wang, W. Han, F. Bian, Z.Q. Liu, S.P. Yan, D.Z. Liao, Z.H. Jiang, P. Cheng. *J. Mol. Struct.*, **733**, 125 (2005).
[48] X.J. Zhao, M. Du, Y. Wang, J.H. Guo, X.H. Bu. *Inorg. Chim. Acta*, **358**, 4481 (2005).
[49] A.W. Addison, T.N. Rao, J. Reedijk, J. van Rijn, G.C. Verschoor. *J. Chem. Soc., Dalton Trans.*, 1349 (1984).
[50] S. Youngme, P. Phuengphai, N. Chaichit, G.A. van Albada, O. Roubeau, J. Reedijk. *Inorg. Chim. Acta*, **358**, 849 (2005).
[51] M.J. Bearpark, K.Y. Seol. *J. Am. Chem. Soc.*, **13**, 3211 (2000).

[52] T. Hirohama, Y. Kuranuki, E. Ebina, T. Sugizaki, H. Arii, M. Chikira, P. Tamil Selvi, M. Palaniandavar. *J. Inorg. Biochem.*, **99**, 1205 (2005).
[53] L. Tian, B. Qian, Y. Sun, X. Zheng, M. Yang, H. Li, X. Liu. *Appl. Organmet. Chem.*, **19**, 980 (2005).
[54] P. Jaividhya, R. Dhivya, M.A. Akbarsha, M. Palaniandavar. *J. Inorg. Biochem.*, **114**, 94 (2012).
[55] A.M. Pyle, J.P. Rehmann, R. Meshoyrer, C.V. Kumar, N.J. Turro, J.K. Barton. *J. Am. Chem. Soc.*, **111**, 3051 (1989).
[56] M. Baldini, M. Belicchi-Ferrari, F. Bisceglie, P.P. Dall'Aglio, G. Pelosi, S. Pinelli, P. Tarasconi. *Inorg. Chem.*, **43**, 7170 (2004).
[57] H.H. Lu, Y.T. Li, Z.Y. Wu, K. Zheng, C.W. Yan. *J. Coord. Chem.*, **64**, 1360 (2011).
[58] X.W. Zhang, Y.J. Zheng, Y.T. Li, Z.Y. Wu, C.W. Yan. *J. Coord. Chem.*, **63**, 2985 (2010).
[59] C.Y. Gao, X.F. Ma, J. Lu, Z.G. Wang, J.L. Tian, S.P. Yan. *J. Coord. Chem.*, **64**, 2157 (2011).
[60] R.K. Bindiya Devi, S. Pramodini Devi, R.K. Bhubon Singh, R.K. Hemakumar Singh, T. Swu, W. Radhapiyari Devi, C.H. Brajakishore Singh. *J. Coord. Chem.*, **67**, 891 (2014).
[61] Y.G. Sun, K.L. Li, Z.H. Xu, T.Y. Lv, S.J. Wang, L.X. You, F. Ding. *J. Coord. Chem.*, **66**, 2455 (2013).
[62] J.R. Lakowicz, G. Weber. *Biochemistry*, **12**, 4161 (1973).
[63] M. Cory, D.D. McKee, J. Kagan, D.W. Henry, J.A. Miller. *J. Am. Chem. Soc.*, **107**, 2528 (1985).
[64] Z.B. Ou, Y.H. Lu, Y.M. Lu, S. Chen, Y.H. Xiong, X.H. Zhou, Z.W. Mao, X.L. Le. *J. Coord. Chem.*, **66**, 2152 (2013).
[65] S. Anbu, A. Killivalavan, E.C.B.A. Alegria, G. Mathan, M. Kandaswamy. *J. Coord. Chem.*, **66**, 3989 (2013).
[66] R.C. Santra, K. Sengupta, R. Dey, T. Shireen, P. Das, P.S. Guin, K. Mukhopadhyay, S. Das. *J. Coord. Chem.*, **67**, 265 (2014).
[67] M.L. Liu, M. Jiang, K. Zheng, Y.T. Li, Z.Y. Wu, C.W. Yan. *J. Coord. Chem.*, **67**, 630 (2014).
[68] T.T. Xing, S.H. Zhan, Y.T. Li, Z.Y. Wu, C.W. Yan. *J. Coord. Chem.*, **66**, 3149 (2013).
[69] C. Icsel, V.T. Yilmaz, A. Golcu, E. Ulukaya, O. Buyukgungor. *Bioorg. Med. Chem. Lett.*, **23**, 2117 (2013).
[70] L.H. Zhi, W.N. Wu, Y. Wang, G. Sun. *J. Coord. Chem.*, **66**, 227 (2013).
[71] M. Ganeshpandian, S. Ramakrishnan, M. Palaniandavar, E. Suresh, A. Riyasdeen, M.A. Akbarsha. *J. Inorg. Biochem.*, **140**, 202 (2014).
[72] N. Shantibala Devi, L. Jaideva Singh, S. Pramodini Devi, R.K. Bhubon Singh, R.K. Hemakumar Singh, B. Rajeswari, R.M. Kadam. *J. Mol. Struct.*, **1076**, 411 (2014).
[73] W.J. Song, Q.Y. Lin, W.J. Jiang, F.Y. Du, Q.Y. Qi, Q. Wei. *Spectrochim. Acta, Part A*, **137**, 122 (2015).
[74] S. Satyanarayana, J.C. Dabrowiak, J.B. Chaires. *Biochemistry*, **32**, 2573 (1993).
[75] P.R. Reddy, A. Shilpa, N. Raju, P. Raghavaiah. *J. Inorg. Biochem.*, **105**, 1603 (2011).
[76] Q.P. Qin, Y.L. Li, Y.C. Liu, Z.F. Chen. *Inorg. Chim. Acta*, **421**, 260 (2014).
[77] Z.Y. Ma, J. Shao, W.G. Bao, Z.Y. Qiang, J.Y. Xu. *J. Coord. Chem.*, **68**, 277 (2015).